ISTANBUL TECHNICAL UNIVERSITY ★ GRADUATE SCHOOL OF SCIENCE

Electromagnetic Form Factors of Ξ_c and Ξ_c' in Lattice QCD

M.Sc. THESIS

Onur Karayalçın

Department of Physics Engineering

Physics Engineering Programme

JUNE 2016

ISTANBUL TECHNICAL UNIVERSITY ★ GRADUATE SCHOOL OF SCIENCE

Electromagnetic Form Factors of Ξ_c and Ξ_c' in Lattice QCD

M.Sc. THESIS

Onur Karayalçın
(509141123)

Department of Physics Engineering

Physics Engineering Programme

Thesis Advisor: Doç. Dr. M. Altan ÇAKIR
Eş Danışman: Doç. Dr. Güray ERKOL

JUNE 2016

İSTANBUL TEKNİK ÜNİVERSİTESİ ★ FEN BİLİMLERİ ENSTİTÜSÜ

Ξ_c ve Ξ_c' Parçacıklarının Elektromanyetik Yapı Faktörünün Örgü Kuantum Renk Dinamiği İle Bulunması

YÜKSEK LİSANS TEZİ

Onur Karayalçın
(509141123)

Fizik Mühendisliği Anabilim Dalı

Fizik Mühendisliği Programı

Tez Danışmanı: Doç. Dr. M. Altan ÇAKIR
Eş Danışman: Doç. Dr. Güray ERKOL

HAZİRAN 2016

Onur Karayalçın, a M.Sc. student of ITU Graduate School of ScienceEngineering and Technology 509141123 successfully defended the thesis entitled "Electromagnetic Form Factors of Ξ_c and Ξ_c' in Lattice QCD", which he/she prepared after fulfilling the requirements specified in the associated legislations, before the jury whose signatures are below.

Thesis Advisor :	**Doç. Dr. M. Altan ÇAKIR** İstanbul Technical University	.....
Co-advisor :	**Doç. Dr. Güray ERKOL** Özyeğin University	.....
Jury Members :	**Prof. Dr. Cenap Şehabettin ÖZBEN** İstanbul Technical University	.....
	Doç. Dr. Ahmet Levent SUBAŞI İstanbul Technical University	.....
	Doç. Dr. Taylan YETKİN Yıldız Technical University	.....

Date of Submission : **02 May 2016**
Date of Defense : **07 June 2016**

To my dear family,

FOREWORD

Firstly, I would like to express my sincere gratitude to my supervisor Assoc. Prof. Dr. Güray Erkol for the continuous support of my master study and related research, for his immense knowledge, motivation and patience. His guidance helped me in all the time of research and writing of this thesis. I am also thankful to Assoc. Prof. M. Altan Çakır for his endless patient, insightful comments and encouragement, but also for the hard question which incented me to widen my research from various perspectives. I thank specially to Hüseyin Bahtiyar for lending assistance me to correct my thesis and stimulating discussions. Besides my supervisors, I would like to thank the rest of my thesis committee: Prof. Dr. Cenap Şahabettin Özben , Assoc. Prof. Dr. Taylan Yetkin and Assoc. Prof. Dr. Ahmet Levent Subaşı for accepting to be a member of my jury.

I want to thank Kadir Utku Can for his sincere guidance and helps. Thanks to İlknur Köseoğlu and Fatih Ilgın for the sleepless nights we were working together before deadlines. Also I thank Asst. Prof. Dr. Bora Işıldak for encouragement and motivating me during writing my thesis. I am grateful to all others who joined at my thesis defense, for their supports.

Last but not the least, I would like to thank my family for supporting me spiritually throughout writing this thesis and my life in general.

We used a modified version of Chroma software system [1]. I thank to The Scientific and Technological Research Council of Turkey (TUBITAK). This work was supported by TUBITAK under project number 114F261.

June 2016

Onur Karayalçın
(Physics Engineer)

TABLE OF CONTENTS

Page

FOREWORD ..... **ix**
TABLE OF CONTENTS ..... **xi**
ABBREVIATIONS ..... **xiii**
LIST OF TABLES ..... **xv**
LIST OF FIGURES ..... **xvii**
SUMMARY ..... **xix**
ÖZET ..... **xxi**
1. CHAPTER 1 ..... **1**
1.1 Introduction 1
2. CHAPTER 2 ..... **5**
2.1 QCD On The Lattice 6
2.2 Discrete Space-Time 9
2.3 Fermionic Action 10
2.4 Gauge Action 12
3. CHAPTER 3 ..... **15**
3.1 Mass Spectrum 15
3.2 Electromagnetic Form Factor 16
3.2.1 Lattice formulation 16
3.2.2 Correlation function and ratio 16
3.3 Techniques For Analyzing Data 18
3.4 Simulation Details 18
4. CHAPTER 4 ..... **21**
4.1 Results 21
4.1.1 Mass spectrum 21
4.1.2 Electric form factor 22
4.1.3 Magnetic form factor 24
4.2 Discussion of Errors 26
5. CONCLUSION **27**
REFERENCES **29**
APPENDICES **33**
APPENDIX A 35
CURRICULUM VITAE **37**

ABBREVIATIONS

LQCD = Lattice Quantum Chromodynamics
SM = Standart Model
QCD = Quantum Chromodynamics
QCDSR = Quantum Chromodynamics Sum Rules
QED = Quantum Electrodynamics
ξ PT = Chiral Perturbation Theory

LIST OF TABLES

Page

Table 1 : Kuarkların temel özellikleri xxi
Table 4.1 : Mass and fit values. 21
Table 4.2 : Magnetic form factor of Ξ_c and Ξ_c' at zero momentum. 25

LIST OF FIGURES

Page

Figure 1.1 : Running of the strong coupling constant, α_S [2]. 2
Figure 1.2 : Significant Lattice QCD results of hadron spectroscopy [3]. 3
Figure 1.3 : Significant Lattice QCD results of the running coupling constant [4]. 3
Figure 1.4 : Resonances of the SU(4) group [5]. 4
Figure 2.1 : The link variables $U_{-\mu}(n)$ and $U_{\mu}(n)$ [6]. 12
Figure 2.2 : The plaquatte of U fields [6]. 13
Figure 3.1 : Diagram of the two and three point correlations [7]. 17
Figure 4.1 : Effective mass plot of Ξ_c, black horizontal line indicates the fit region. 21
Figure 4.2 : Effective mass plot of Ξ_c', black horizontal line indicates the fit region. 22
Figure 4.3 : Electric form factor of $\Xi_c(dsc)$. 22
Figure 4.4 : Electric form factor of $\Xi_c'(dsc)$. 23
Figure 4.5 : Electric form factor of $\Xi_c(usc)$. 23
Figure 4.6 : Electric form factor of $\Xi_c'(usc)$. 23
Figure 4.7 : Magnetic form factor of $\Xi_c(dsc)$. 24
Figure 4.8 : Magnetic form factor of $\Xi_c'(dsc)$. 24
Figure 4.9 : Magnetic form factor of $\Xi_c(usc)$. 25
Figure 4.10 : Magnetic form factor of $\Xi_c'(usc)$. 25
Figure A.1 : Linear mass plot of Ξ_c. 35
Figure A.2 : Mass spectrum plot of Ξ_c. 35
Figure A.3 : Linear mass plot of Ξ_c'. 36
Figure A.4 : Mass spectrum plot of Ξ_c'. 36

Electromagnetic Form Factors of Ξ_c and Ξ_c' in Lattice QCD

SUMMARY

The Standard Model (SM) is the theory to explain the strong, electromagnetic and weak forces and the interactions among all fundamental particles in nature. In order to understand the dynamics of these fundamental forces, there are a number of methods. One of the most successful theories is the Lattice Quantum Chromodynamics (LQCD). The method uses the Lattice Gauge Theory in the theoretical background. Furthermore, the Lattice Quantum Chromodynamics is not based on any approximate or effective model and it uses computational techniques effectively to make calculations. Lattice Gauge Theory is utilized with improvements in computational techniques and high-technology provides golden opportunities to compute the action of Quantum Chromodynamics (QCD) precisely. Electromagnetic form factors provide significant knowledge for understanding composite structure of baryons. Additionally, charmed baryons are an attractive field to investigate fundamental mechanism behind hadron structure. The charmed baryons are compact particles as compared to the proton. In this work, our aim is to compute the electromagnetic form factors of singly charmed Ξ_c and Ξ_c' baryons from 2+1-flavor simulations of QCD. The bound states of two light (up and strange) and one heavy (charm) quark regime is very significant to obtain baryon structure and properties. We define a ratio to calculate the electromagnetic form factor and magnetic moment. We express our results of the mass spectrum of Ξ_c and Ξ_c' as simulated on $16^3 \times 32$ lattices. We make the statistical analysis of data. We calculate magnetic moments of charmed baryons and discuss individual contribution of quarks to baryon structure. The magnetic moments of singly charmed baryons are found to be dominantly determined by the light quark contribution in aligned spin state of the light quarks. The role of the charm quark effects are mainly explicit when spins of the light quarks are anti-aligned. Our results also indicate that the singly charmed baryons have compact structure as compared to proton which consists of only light quarks.

Ξ_c ve Ξ_c' Parçacıklarının Elektromanyetik Yapı Faktörünün Örgü Kuantum Renk Dinamiği İle Bulunması

ÖZET

Standart Model güçlü, elektromanyetik ve zayıf kuvvetleri açıklamak için geliştirilmiş bir teoridir. Bu temel kuvvetler doğada atomaltı ölçekte meydana gelen olayların ve etkileşimlerin gerçekleşmesini sağlar. Standart Model çerçevesinde parçacıklar kütleli olarak ele alınmasına rağmen, parçacıklar arasında kütleçekimsel etkileşimlerin olmadığı varsayılır. Standart Model, parçacıkların davranışını açıklayabilmesine karşın eksiklikleri olan bir teori olarak karşımıza çıkar ve günümüzde pek çok araştırma Standart Model ötesi teoriler adı altında yürütülmektedir.

Kuantum Renk Dinamiği, kuark ve gluon parçacıkları arasındaki etkileşimleri açıklar. Kuarklar, Fermi-Dirac istatistiğine uyan ve yarım-katlı spin yapısına sahip olan maddesel parçacıklar ve gluonlar ise kuarkların birbirleriyle etkileşmesini sağlayan aracı parçacıklar olarak karşımıza çıkar. Gluonlar, Bose-Einstein istatistiksel dağılımına uyan ve tam-katlı spin yapısına sahip olan parçacıklardır. Kuarkların çeşnileri altı tanedir ve bu kuarkların kütleleri de farklı olduğundan dolayı hafif ve ağır kuarklar olmak üzere iki sınıfta toplanırlar. Yukarı (up), aşağı (down) ve acayip (strange) kuarklar hafif; tılsım (charm), alt (bottom) ve üst (top) kuarklar ise ağır olarak incelenirler. Kuarkların özellikleri Table 1.' de gösterilmiştir. Gluon ise kütlesiz ve elektriksel olarak nötr bir parçacık olarak karşımıza çıkar.
e* : elektronun elektrik yükü

Table 1 : Kuarkların temel özellikleri

kuark	kütle	elektrik yük (e*)
yukarı	$2.3^{+0.7}_{-0.5}$ MeV	$(2/3)$e
aşağı	$4.8^{+0.5}_{-0.3}$ MeV	$(-1/3)$e
acayip	95 ± 5 MeV	$(-1/3)$e
tılsımlı	1.275 ± 0.025 GeV	$(2/3)$e
alt	4.18 ± 0.03 GeV	$(-1/3)$e
üst	173.21 ± 0.51 GeV	$(2/3)$e

Bu teoriye Kuantum Renk Dinamiği adı verilmesi, nükleon içerisinde bulunan kuark ve gluonların renk yükü taşımalarından dolayıdır. Renk yüküne sahip olan parçaçıklar birbirleriyle bu renk yükleri sayesinde etkileşirler. Tıpkı Mawxell'in Klasik Elektromanyetik Alan Teorisi'nde olduğu gibi bu renk yüklerinin oluşturduğu renk manyetik alanları da vardır. Gluonlar aracı parçacıklar oldukları için iki adet ve kuarklar tek adet renk yükü taşırlar. Günümüze kadar, henüz hiçbir deneyde serbest halde gluon yada kuarka rastlanmamıştır. Üstel serbestlik (asymptotic freedom)

adı verilen ilişki sonucunda renk yükü taşıyan parçacıkların gözlenebilir olması için singlet dalga fonksiyonuna sahip olması gerekir. Hadronlar iki alt ana başlıkta incelenirler: baryonlar ve mezonlar. Baryonlar üç adet kuarka sahip parçacıklardır ve her kuark kırmızı, yeşil ve mavi olmak üzere üç ana renk yükünü taşırlar. Bundan dolayı renksiz parçacıklardır. Mezonlar ise, kuark-anti kuark çiftini taşıdıkları için hangi renk yükünün kuarklar tarafından taşındığının bir önemi olmaksızın singlet parçacıklar olarak oluşurlar.

Güçlü etkileşimlerde, çiftlenim sabiti α_S bu kuvvetin karakteristik özelliklerinin anlaşılması bakımından çok önemli bir yere sahiptir. Çünkü bu sabit sayesinde gerçekleşen olaylar ve etkileşim türlerinin doğası anlaşılabilir. Çiftlenim sabiti ise enerjiye bağlı olarak değişen bir karaktere sahiptir. Yüksek enerjilerde momentum transferi yüksek olduğundan, çiftlenim sabitinin değeri azalırken, düşük enerjilerde ise artar. Diğer bir deyişle, çiftlenim sabiti düşük enerjilerdeki küçük değişimlerin etkilerinin ihmal edilebildiği bir davranış gösterirken, yüksek enerjilerde çiftlenim sabiti görece daha da zayıfladığı için enerjideki küçük değişimlerin etkileri ihmal edilemez sonuçlar ortaya çıkartabilir. Yani hadron içerisinde bağlı durumda olan kuarkların arasındaki etkileşme potansiyel enerjisi, Kuantum Elektrodinamiği'ne göre doğrusal olmayan bir davranışa sahiptir. Bu etkileşme potansiyeli, lineer, lineer olmayan ve sabit terimleri içerisinde barındırır. Bunların hepsi güçlü ve elektromanyetik etkileşmelerden kaynaklıdır.

Kuantum Renk Dinamiği, üstel serbestlik, güçlü etkileşmelerin çiftlenim sabiti ve genel itibariyle kuark dinamiğini iyi anlamak üzere geliştirilmeye devam edilmektedir. Bu konuda, özellikle charm kuarkların oluşturduğu bağlı durumlar ve geçişlerin sonuçları önem arz etmektedir. Çünkü charm kuark bağlı duruma geçebilen ağır kuarklardan birisidir. Charm sektörün bu özelliği oldukça ilgi çekici ve merak uyandırıcıdır. Bu yüzden çalışmamızda Ξ_c ve Ξ_c' baryonlarının fiziksel bir takım özelliklerinin irdelenmesine ve bulunmasına yer verdik.

Kuantum Renk Dinamiği'nin anlaşılması adına geliştirilen metotlardan bir tanesi de Örgü Kuantum Renk Dinamiğidir. Güçlü çiftlenim sabitinin düşük enerjilerde daha büyük değere sahip olmasından dolayı pertürbatif olmayan fiziksel yöntemler esas alınır. Formülasyon ve teorik altyapı olarak Örgü Ayar Kuramını kullanır. Model bağımsız bir yöntem olmasından dolayı analitik çözümlerle çok yakın sonuçlar vermektedir. Hesaplamalar temel olarak kuark ve gluon alanlarının, dört boyutlu uzay-zamanda, bir hiperküp üzerine yerleştirilerek bu yapının çözülmesine dayanmaktadır. Bu hesaplamalar, süper hızlı bilgisayarlar yardımıyla ve paralel hesaplama yöntemleri kullanılarak gerçekleştirilir. GPU grafik kartlarının geliştirilmesi bu alana büyük katkılar sağlamıştır. Bundan dolayı, bu yöntemin en büyük dezavantajı hesaplamaların yapılması adına süper bilgisayarlara ihtiyaç duyulması olarak kabul edilebilir. Hesaplama bilgisayar ortamında yapıldıktan sonra elde edilen veriler analiz edilirken Jackknife metodu kullanılır. Bu yöntem birbirinin ardışığı olarak alınan veriler arasındaki ilintiden (correlation) ötürü hataları (bias) birbirlerine aktarılır. Neticede, bir konfigürasyon içinde alınan en son verilerin hata miktarı çok yüksektir ve yanlış sonuçlara ulaşılmasına sebep olur. Bunun önüne geçmek adına Jaccknife analizi yapılır ve yeni örnek veriler üzerinden hesaplamalar yapılır.

Ξ_c ve Ξ_c' baryonları aynı kuarkları (u, s ve c) içermelerine rağmen, bu kuarkların

spin yönelimleri farklıdır. Charm kuark her iki bağlı durumda spin-up durumunda bulunmasına rağmen; s ve u kuarkların spin yönelimleri paralel spin-down yada anti-paralel olarak bulunurlar. Spin konfigürasyonlarındaki bu farklılık parçacıkların farklı kütle kazanmalarını sağlar. Spin-spin etkileşmelerinin Kuantum Mekaniksel hesaplamaları, aşırı ince yapı yarılması adı altında bize bu kütle farkını verir.

Yüksek Enerji Fiziği'nde, parçacıkların önemli özelliklerinden bir tanesi de form faktörüdür. Parçacığın hadronik yapısının ve girebileceği etkileşmelerin anlaşılmasında kilit bir görevi vardır. Form faktörü, elektrik ve manyetik form faktörü olmak üzere ikiye ayrılır. Aynı zamanda, parçacıkların yapabilecekleri saçılmala türleri ve bu saçılmaların tesir kesitlerinin hesaplanması için de büyük önem teşkil etmektedir. Ayrıca parçacıklar arasında olan veyahut aynı parçacığın farklı kuantum mekaniksel durumları arasındaki geçişleri de yine form faktör hesabını yaparak anlayabiliriz. Ξ_c ve Ξ_c' baryonlarının ise form faktörleri arasında, kuark dizilimleri ve çeşnileri aynı olmasına karşın spin konfigürasyonunda olan değişiklikten dolayı, fark ortaya çıkmaktadır. Ayrıca sıfır momentum durumlarında, elektrik form faktörü elektrik yükünü verirken, manyetik form faktörü ise manyetik moment değerine ulaşmamızı sağlar. Bu iki fiziksel özellik bir parçacık için temel yapısal karakteristiklerdendir.

1. CHAPTER 1

1.1 Introduction

The Standard Model (SM) is the theory of three of the four fundamental forces which are basics of particle physics. These are the strong, electromagnetic and weak forces when they are compared to strength of interaction. The three forces have significant roles to understand concept of nature. We are able to handle the SM as a gauge theory with gauge groups of the three forces. Namely, the U(1) $\times$ SU(2)$_L$ group is used to express physical events related to the electroweak interaction, the SU(3) group reveals the dynamics of strong interaction. The model is unification of all the expressed groups. On the other hand, the gravitational force is not included in the SM, due to the fact that there is no proof for mediator particle of gravity which is called graviton.

The elementary particles are divided into two groups which are called Fermions and Bosons. The Bose particles have integer spin (e.g. 0,1,2, ...) and carry interaction of fundamental forces among the Fermions. However, the Fermions are grouped as quarks and leptons and their spins are half-integer (e.g. 1/2, 3/2, ...).

If we concentrate on strong interactions, the quarks and gluons are the only particles to interact with this force. Except electric charge and spin numbers, these two particles carry a new quantum number called the color charge. Hence, Quantum Chromodynamics (QCD) arises from the color concept. One peculiarity of the strong interaction (QCD) is different behavior of the strong coupling constant (α_S) than the fine structure constant (α) in Quantum Electrodynamics . α_S is decreasing with increasing energy whereas α is not. This behavior is known as *asymptotic freedom* and it allows us to make calculations perturbatively in the high energy regime. Behavior of strong coupling constant (α_s) is shown in Figure 1.1 and Figure 1.3, according to experimental and lattice QCD results. Both of the figures overlap substantially with each other. In experiments of particle physics, we can observe all leptons and bosons, except the particles that interact with strong forces. Up to now, no free quarks or gluons

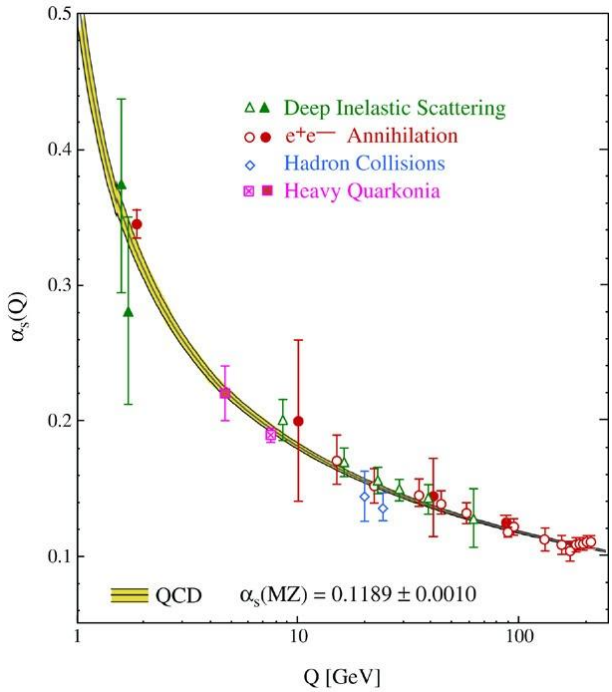

Figure 1.1 : Running of the strong coupling constant, α_S [2].

have been detected. It is speculated that the potential consisting of interaction between the quarks and gluons or self-interaction of gluons are responsible for this peculiar phenomenon. This implies that the composite particles can be observed, provided that they have a *color singlet* wave function which means *colorless*. The composite particles are called hadrons which are classified as baryons and mesons. The baryon sector has three quarks and the mesons have quark-anti-quark pair in it. Ultimately, the hadrons are colorless particles in terms of their inner color structure.

On the other hand, performed experiments for understanding the hadron structure give signals to prove that the quarks are fundamental objects although no single quark has been detected yet. However, investigations about inner structure of hadrons not only provide an insight into its fundamental properties (spin distribution, electric charge, etc.) but also estimate the parameters related to decays and transitions. If we consider bound state of quarks as hadrons, perturbation theory is not efficient to explain dynamics of quarks at small momentum transfers. Because of the non-linear running of the strong coupling constant, non-perturbative QCD effects become apparent [8].

Some methods have been developed to understand the hadron structure theoretically as the QCD Sum Rules (QCDSR) [9, 10] and Chiral Perturbation Theory (ξPT) [11, 12], which are used in the non-perturbative region [12]. There is another encouraging

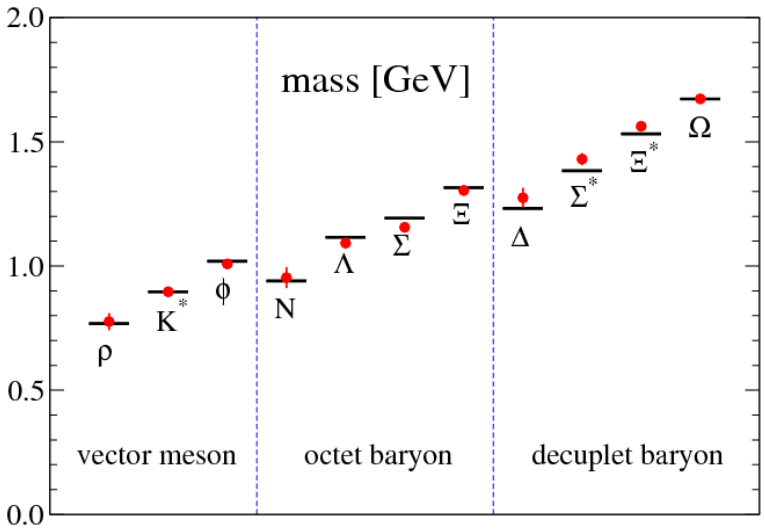

Figure 1.2 : Significant Lattice QCD results of hadron spectroscopy [3].

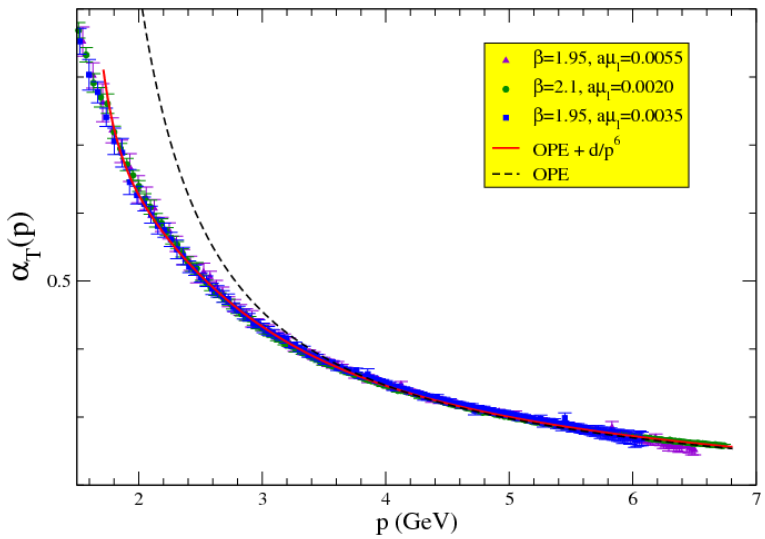

Figure 1.3 : Significant Lattice QCD results of the running coupling constant [4].

non-perturbative method called Lattice QCD (LQCD) [13–15]. The method starts with formulating the QCD Lagrangian by discretizing space-time on a 4D-grid in order to solve it numerically and theoretically. Hence, the method is called an *ab inito* method. LQCD has proved to be an effective method and has become prominent over years with algorithmic and technological development. It has been succesfully used to understand the behavior running coupling constant [4, 16] and the accurate spectroscopy measurements consistent with experimental results [17], as denoted by Figure1.2. Lattice groups achieved convincing advancements to understand the hadron structure. As a result, LQCD has brought improvements to other methods in particle physics.

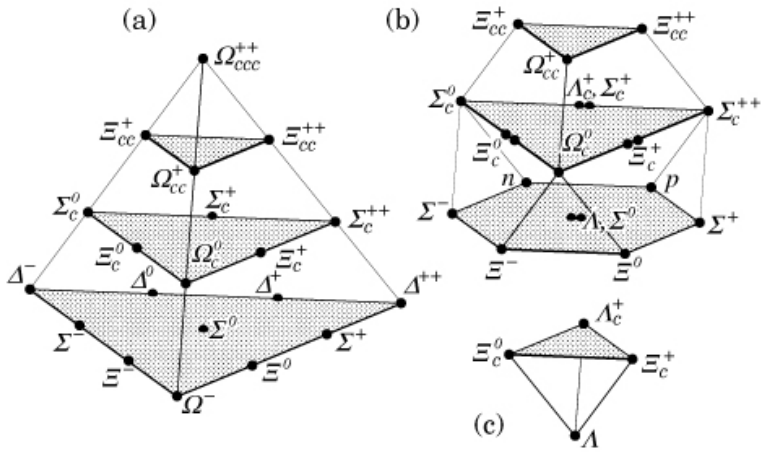

Figure 1.4 : Resonances of the SU(4) group [5].

The understanding of behavior of the heavy quarks (t, b, c) and light quarks (s, d, u) attract a lot of interest to the mentioned non-perturbative methods [18, 19]. Moreover, there are still some properties of charm sector which should be determined from LQCD [20, 21]. However, it is anticipated that the charm sector is going to give clues for realizing some secrets of the quark-gluon plasma state. Hence, the Ξ_c and Ξ_c' baryons are significant particles for heavy quark physics.

Spin configuration of the Ξ_c and Ξ_c' baryons are arranged differently though they consist of u, s and c quarks basically, in two light and one heavy quark regime. The hyper-fine structural effect of u and s quarks results in splitting of their masses into two values [22–24]. Spin-3/2 baryons are included in Figure1.4.a whereas spin-1/2 baryons are indicated in Figure 1.4.b and in Figure 1.4.c. However, (usc) and (dsc) combinations of the Ξ_c' state at midsection of twenty-plet subgroup in Figure 1.4.b. Four-plet subgroup possesses (usc) and (dsc) combinations of the Ξ_c baryon on upper side of Figure 1.4.c.

Organization of this thesis is as follows; we describe theoretically the LQCD method to explain how to discretize the QCD action in continuum and space-time in chapter 2. The simulation technique and analysis of data are obtained in chapter 3. We express our results and the sources of errors in chapter 4. We interpret results of the calculations in chapter 5.

2. CHAPTER 2

In lattice QCD, derived equations should be regularized in order to extract some physical information. Using the correlation function which describes behaviors of quarks in quantum field theory, we obtain values of observable quantities. However, quarks in a hadron are considered as one composite particle quantum mechanically. Hence, these formulations give the same result. Throughout this chapter, we will use Gattringer & Lang's notation [6]. The energy value of such a hadron can be found using :

$$\lim_{T\to\infty}\langle O_2(t)O_1(0)\rangle_T = \sum_n \langle 0|\hat{O}_2|n\rangle\langle n|\hat{O}_1|0\rangle e^{-tE_n}. \tag{2.1}$$

Also, it can be written in the path integral formalism:

$$\langle \hat{O}_2(t)\hat{O}_1(0)\rangle = \frac{1}{Z_T}\int D[\Psi]e^{-S_E[\Psi]}O_2[\Psi(\vec{x},t)]O_1[\Psi(\vec{x},0)], \tag{2.2}$$

$$D[\Psi] = \prod_{n\in\Lambda} d[\Psi(x)], \tag{2.3}$$

$$Z_T = \int D[\Psi]e^{-S_E[\Psi]}. \tag{2.4}$$

where $\hat{O}_2(t)$ and $\hat{O}_1(0)$ are the Euclidean operators , $\wedge$ is 4D lattice space and n denotes lattice point in the $\wedge$, E_n is the energy of the hadronic state, $S_E[\Psi]$ is discretized action and Z_T is the partition function. $\hat{O}_1(0)$ operator creates any related particles from the vacuum state ($|0\rangle$) and $\hat{O}_2(t)$ operator causes to annihilation of the created particle at time t. However, operations of these operators carry both ground state and excited states contributions with them. In this way, a production-annihilation process of an

hadronic state on lattice is completed.

In order to solve the correlation function by numerical methods, it is so useful to transform correlation relation into Euclidean space from Hilbert space. So, it is possible by doing *Wick rotation*. Besides, there are two beneficial results of such a rotation. First of all, characteristic of weight factor e^{-S_E} is changed to be a well-behaved function into Euclidean space, it is not oscillating sharply as in Hilbert space. Second one is such rotation gives us some resemblance between *quantum field theories* and *statistical field theories* and it allows the utilization of some statistical techniques like *Monte Carlo methods*, which e^{S_E} is accepted weight factor.

In the following sections we explain *the QCD action in the continuum, naive discretization of fermions, Wilson gauge action* and improved discretization methods in this work.

2.1 QCD On The Lattice

The form of QCD action in continuum is as noted below:

$$S[\Psi,\bar{\Psi},A] = \sum_{f=1}^{N_f} \int d^4x \bar{\Psi}^{(f)}(x)_{\alpha c}[\gamma_\mu(\partial^\mu + igA^\mu(x)) + m^{(f)}]\Psi^{(f)}(x)_{\alpha c} + \frac{1}{2}\int d^4x \mathrm{Tr}[F_{\mu\nu}F^{\mu\nu}], \tag{2.5}$$

where $\bar{\Psi}^{(f)}(x)_{\alpha c}, \Psi^{(f)}(x)_{\alpha c}$ are the anti-fermion and fermion spinors respectively. Also, α, c, f are Dirac, color and flavor indexes relatively. $A_\mu(x)$ is the gauge field, g is the strong coupling constant and μ denotes Lorentz index ($\mu = 1,2,3,4$), A_μ is gauge field and γ_μ is called Dirac matrices which obey the Euclidean anti-commutation relation,

$$\{\gamma_\mu, \gamma_\nu\} = 2\delta_{\mu\nu}\mathbb{I}, \tag{2.6}$$

where $\mathbb{I}$ is identity matrix. As a result of switching between Minkowski and Euclidean spaces, we encounter the following relation,

$$\gamma_1 = -i\gamma_1^M, \gamma_2 = -i\gamma_2^M, \gamma_3 = -i\gamma_3^M, \gamma_4 = -i\gamma_0^M, \tag{2.7}$$

where the $\gamma_1 = -i\gamma^M_{0,1,2,3}$ matrices are presented in Minkowski space. $F_{\mu\nu}$ is the field strength tensor,

$$F_{\mu\nu} = \partial_\mu A_\nu(x) - \partial_\nu A_\mu(x) + i[A_\mu(x), A_\nu(x)]. \tag{2.8}$$

The action is derived for a single flavor of quarks since flavour number f varies from 1 to 6. Having discussed our notation in detail, it can be said that the action describes the relativistic wave equation for fermions by taking account of Dirac Lagrangian density. Additionally, different flavours have different electric charges, hence couple to the different electromagnetic fields. After all, we just describe the strong interaction fields.

In electrodynamics, the action of fermionic fields is invariant at any space-time point x. In QCD, we require the action should be invariant under local rotations among the color indeces of the quarks with making an analogy to QED. At each space-time point x we choose an independent complex 3×3 matrix $\Omega(x)$. The matrix is not only unitary but also $\det[\Omega(x)] = 1$ value. These type of matrices are defined as *special unitary group* by SU(3). Turning back to obtain our expression of the QCD gauge invariance, it is required that invariance of the action must be provided under the transformations:

$$\Psi(x) \longrightarrow \Psi(x)' = \Omega(x)\Psi(x), \tag{2.9}$$

$$\bar{\Psi}(x) \longrightarrow \bar{\Psi}(x)' = \bar{\Psi}(x)\Omega(x)^\dagger. \tag{2.10}$$

When the transformation terms are put into the fermion action, it may be seen easily that A_μ field represented as

$$A_\mu(x) \longrightarrow A_\mu(x)' = \Omega(x)A_\mu(x)\Omega(x)^\dagger + i(\partial_\mu\Omega(x))\Omega(x)^\dagger. \tag{2.11}$$

Note that here A_μ is traceless and hermitian as expected for gauge fields. The gauge part of action is constructed by defining the covariant derivative to provide invariance

under local transformations. The covariant derivative defined as

$$D_\mu(x) \longrightarrow D_\mu(x)' = \partial_\mu + iA_\mu(x)' = \Omega(x)D_\mu(x)\Omega(x)^\dagger. \tag{2.12}$$

Now we identify field strength tensor $F_{\mu\nu}(x)$ as the commutator

$$F_{\mu\nu} = -i[D_\mu(x), D_\nu(x)] = \partial_\mu A_\nu(x) - \partial_\nu A_\mu(x) + i[A_\mu(x), A_\nu(x)]. \tag{2.13}$$

Additionally, the field strength tensor ensure transformation properties as

$$F_{\mu\nu}(x) \longrightarrow F_{\mu\nu}(x)' = \Omega(x)F_{\mu\nu}\Omega(x)^\dagger. \tag{2.14}$$

As a result, we express the gluon action in terms of the field strength tensor:

$$S_G[A] = \frac{1}{2g^2}\int d^4x tr[F_{\mu\nu}(x)F^{\mu\nu}(x)], \tag{2.15}$$

$$D_\mu(x) \longrightarrow \partial_\mu + igA_\mu(x). \tag{2.16}$$

In the covariant derivative term, g denotes coupling strength of gauge fields to the quarks. $A_\mu(x)$ indicates gauge fields as traceless and hermitian matrices. It obeys SU(3) group properties which presented by

$$A_\mu(x) = \sum_{i=1}^{8} A_\mu^{(i)}(x)T_i, \tag{2.17}$$

where T_i become a basis for traceless, hermitian 3×3 matrices and components of $A_\mu^{(i)}(x), i = 1, 2, ..., 8$, are real-valued fields which is assumed color components. Inserting (2.17) into (2.13), then we obtain

$$F_{\mu\nu} = \sum_{i=1}^{8}(\partial_\mu A_\nu^{(i)}(x) - \partial_\nu A_\mu^i(x))T_i + i\sum_{j,k=1}^{8} A_\mu^{(j)}(x)A_\nu^{(k)}(x)[T_j, T_k]. \tag{2.18}$$

By simplifying the commutator relation is obtained and it ends up with

$$F_{\mu\nu} = \sum_{i=1}^{8} F_{\mu\nu}^{(i)}(x) T_i, \tag{2.19}$$

$$F_{\mu\nu}^{(i)} = \partial_\mu A_\nu^{(i)}(x) - \partial_\nu A_\mu^{(i)}(x) - f_{ijk} A_\mu^{(j)}(x) A_\nu^{(k)}(x), \tag{2.20}$$

where f_{ijk} is called structure constant. The field strength is calculated now in more explicit form which we can see easily interactions between gluons. The gluonic action can be written in a compact form in order to evaluate the trace of gauge action. The equation arises that

$$S_G[A] = \frac{1}{4g^2} \sum_{i=1}^{8} \int d^4x F_{\mu\nu}^{(i)}(x) F_{\mu\nu}^{(i)}(x). \tag{2.21}$$

From this equation, we extract that the gluonic action is a sum over all color components. Furthermore, the interaction term resembles the action of electrodynamics and it supplies some benefical results to make an analogy between strong and electromagnetic interactions. On the other hand, a qualitatively new feature of field strength glitters that color components do not act linear because of the gauge field $A_\mu^{(i)}(x)$. However, cubic and quartic gluon self-interactions emerge from being mixed the varied color components of the gluon field. Hence, we encounter not only quadratic terms like being in electrodynamics but also cubic and quartic term as a result of gluonic interactions. Additionally, these gluonic self-interactions causes confinement of the color, the most outstanding property of QCD.

2.2 Discrete Space-Time

Firstly, we switch the continuum space to 4D lattice space $\wedge$:

$$n \in \Lambda = (n_1, n_2, n_3, n_4) \ \mid \ n_1, n_2, n_3 = 0, 1, ..., N-1 \ ; \ n_4 = 0, 1, ..., N_t - 1 \tag{2.22}$$

where N is the total number of the spatial steps and N_T is the total number of the time

steps. Also, $n \in \wedge$ denotes point in space-time splitted by a lattice constant a and actual physical space-time point $x = na$ is not used to specify the lattice position of the quark,

$$\Psi(x) \to a^{-3/2}\Psi(an), \qquad \bar{\Psi}(x) \to a^{-3/2}\bar{\Psi}(an). \tag{2.23}$$

The so-called *Link Variables* U_μ are substituted by the gauge fields of the continuum theory to provide connection between two lattice sites. Besides, they belong to the $SU(3)_c$ group and enable to make transition from one color component to another one with a probability density of related color components. The transition matrix is expressed by;

$$U_\mu = \begin{pmatrix} U_\mu^{rr} & U_\mu^{rg} & U_\mu^{rb} \\ U_\mu^{gr} & U_\mu^{gg} & U_\mu^{gb} \\ U_\mu^{br} & U_\mu^{bg} & U_\mu^{bb} \end{pmatrix}. \tag{2.24}$$

There is a relation between link variables and the continuum fields as follows:

$$U_\mu(x) = \exp(iaA_\mu(n)). \tag{2.25}$$

Another important point here is to reduce infinite space-time to a finite hyper cube construction. It is provided by periodic boundary conditions instead of anti-periodic boundary conditions because discrete translational symmetries must be conserved.

$$\begin{aligned} \Psi(0,n_2,n_3,n_4) &= \Psi(N,n_2,n_3,n_4) \\ &\vdots \\ \Psi(n_1,n_2,n_3,0) &= \Psi(n_1,n_2,n_3,N_T). \end{aligned} \tag{2.26}$$

2.3 Fermionic Action

The fermionic part $S_F[\Psi,\bar{\Psi},A]$ of the QCD is bilinear functional in the fields Ψ and $\bar{\psi}$. It is represented by

$$S_F^0[\Psi,\bar{\Psi}] = \int d^4x \bar{\Psi}(x)(\gamma_\mu \partial_\mu + m)\Psi(x). \tag{2.27}$$

Here, we set the gauge field $A_\mu(x) = 0$ since it is a free fermion action. For our purpose, this action must be discretized on the lattice with the integral over space-time as well as the partial derivative. The integral term is replaced with a sum over $\wedge$ and the partial derivative can be separated with the symmetric expression given by

$$\partial_\mu \Psi(x) \rightarrow \frac{1}{2a}(\Psi(n+\hat{\mu}) - \Psi(n-\hat{\mu})). \tag{2.28}$$

Ultimately, we end up with the fermionic action in a form with

$$S_F^0[\Psi,\bar{\Psi}] = a^4 \sum_{n\varepsilon\lambda} \bar{\Psi}(n)(\sum_{\mu=1}^{4} \gamma_\mu \frac{\Psi(n+\hat{\mu}) - \Psi(n-\hat{\mu})}{2a} + m\Psi(n)). \tag{2.29}$$

In lattice QCD, we introduced that the action must be invariant in continuum. Afterwards, we struggled to discretize the fermionic part of action. However, we should implement the same procedure as being in (2.9) to find out it is gauge invariant or not. When we skip from site n to $n+\hat{\mu}$, consider the term,

$$\bar{\Psi}(n)\Psi(n+\hat{\mu}) \longrightarrow \bar{\Psi}'(n)\Psi'(n+\hat{\mu}) = \bar{\Psi}(n)\Omega^\dagger(n)\Omega(n+\hat{\mu})\Psi(n+\hat{\mu}). \tag{2.30}$$

This term does not provide gauge invariance. Provided that a modified field $U_\mu(n)$ emerges with a directional index $\hat{\mu}$, then

$$\bar{\Psi}(n)\Omega^\dagger(n)U'_\mu(n)\Omega(n+\hat{\mu})\Psi(n+\hat{\mu}) \tag{2.31}$$

is gauge invariant. If we describe the gauge transformations in terms of new field by

$$U_\mu(n) \longrightarrow U'_\mu(n) = \Omega(n)U'_\mu(n)\Omega(n+\hat{\mu})^\dagger. \tag{2.32}$$

After having explained gauge invariance of the link variables and their properties, now we can generalize the free fermion action which is so-called *naive fermion action* in an external gauge field U :

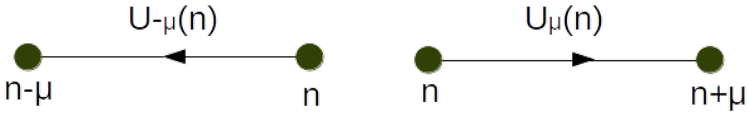

Figure 2.1 : The link variables $U_{-\mu}(n)$ and $U_{\mu}(n)$ [6].

$$S_F^0[\Psi,\bar{\Psi},U] = a^4 \sum_{n\varepsilon\lambda} \bar{\Psi}(n)(\sum_{\mu=1}^{4} \gamma_\mu \frac{U_\mu(n)\Psi(n+\hat{\mu}) - U_{-\mu}(n)\Psi(n-\hat{\mu})}{2a} + m\Psi(n)). \tag{2.33}$$

If we recall the definition of $U_\mu(n)$ field in equation (2.25), we can make the Taylor expansion with respect to A field. We then obtain,

$$U_\mu(n) = 1 + iaA_\mu(n) + \mathscr{O}(a^2), \tag{2.34}$$

$$U_\mu(n-\hat{\nu})^\dagger = 1 - iaA_\mu(n-\hat{\nu}) + \mathscr{O}(a^2), \tag{2.35}$$

$$A_\mu(n-\hat{\mu}) = A_\mu(n) + \mathscr{O}(a), \tag{2.36}$$

$$\Psi(n \pm a) = \Psi(n) + \mathscr{O}(a). \tag{2.37}$$

When we rewrite the fermionic action by embedding the link variables with error $\mathscr{O}(a)$,

$$S_F[\Psi,\bar{\Psi},U] = a^4 \sum_{n\varepsilon\wedge} \sum_{\mu=1}^{4} \bar{\Psi}(n)(\gamma_\mu \partial_\mu + m)\Psi(n) + ia^4 \sum_{n\varepsilon\wedge} \sum_{\mu=1}^{4} \bar{\Psi}(n)\gamma_\mu A_\mu(n)\Psi(n) + \mathscr{O}(a). \tag{2.38}$$

Note that sum over all lattice points added a term proportional $1/a^4$.

2.4 Gauge Action

Here, we use the gauge fields $U_\mu(n)$ as basis of the gauge group SU(3) so that it is gauge invariant. These variables have a matrix kind form and connect two different sites on a lattice.

The link variables can be chosen in negative direction of μ because they are not independent of orientation. Moreover, negative oriented and positive oriented link variables are relevant to each other which means one is able to be written in terms of another one.

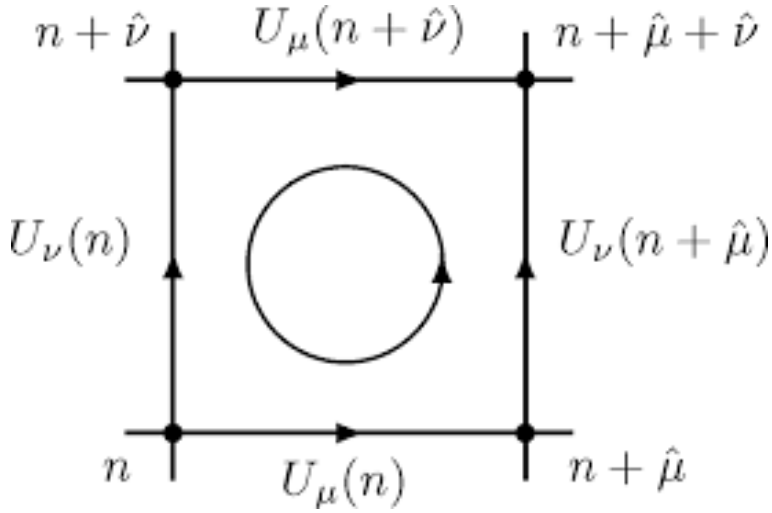

Figure 2.2 : The plaquatte of U fields [6].

$$U_{-\mu}(n) \equiv U_\mu(n-\hat{\mu})^\dagger, \tag{2.39}$$

the transformation specialty of the link in negative direction

$$U_{-\mu}(n) \longrightarrow U'_{-\mu}(n) = \Omega(n)U'_{-\mu}(n)\Omega(n+\hat{\mu})^\dagger. \tag{2.40}$$

On the other hand, in consideration of physical value of $F_{\mu\nu}$, we are able to produce a compact object is called *plaquette* variable $U_{\mu\nu}(n)$ which defined as follows:

$$U_{\mu\nu}(n) = U_\mu(n)U_\nu(n+\hat{\mu})U_\mu(n+\hat{\nu})^\dagger U_\nu(n)^\dagger. \tag{2.41}$$

In this expression, we used the equivalence (2.39). Using the plaquette definition we can write the *Wilson gauge action* as,

$$S_G[U] = \frac{\beta}{3}\sum_{n\varepsilon\wedge}\sum_{\mu<\nu}\mathrm{Re}[\mathrm{Tr}[I-U_{\mu\nu}(n)]], \tag{2.42}$$

where β is called the lattice coupling and it equals to $\beta = 6/g^2$. When we take naive limit of the Wilson action ($a \to 0$), it actually approximates the continuum form. In order to obtain easily resultants of the four link variables in the plaquatte, it is suitable to use the Baker-Campbell-Hausdorff formula for the resultant of exponential of matrices :

$$\exp(A)\exp(B) = \exp(A + B + \frac{1}{2}[A,B] + ...), \tag{2.43}$$

substituting the plaquatte in A and B arbitrary matrices,

$$\begin{aligned} U_{\mu\nu} = \exp\Bigg(& iaA_\mu(n) + iaA_\nu(n+\hat{\mu}) - \frac{a^2}{2}[A_{\mu(n)}, A_\nu(n+\hat{\mu})] \\ & -iaA_\mu(n+\hat{\nu}) - iaA_\nu(n) - \frac{a^2}{2}[A_\mu(n+\hat{\nu}), A_\nu(n)]) \\ & +\frac{a^2}{2}[A_\nu(n+\hat{\mu}), A_\mu(n+\hat{\mu})] + \frac{a^2}{2}[A_\mu(n), A_\nu(n)] \\ & +\frac{a^2}{2}[A_\mu(n), A_\mu(n+\hat{\nu})] + \frac{a^2}{2}[A_\nu(n+\hat{\mu}), A_\nu(n)] + \mathscr{O}(a^3)\Bigg). \end{aligned} \tag{2.44}$$

3. CHAPTER 3

3.1 Mass Spectrum

The hadron correlators serve as a useful tool to calculate mass spectrum of the corresponding hadron. When analyzing the hadron correlators, E, P and m are multiplied by lattice constant a to make these physical quantities dimensionless.

In analysis of hadron mass, an operator $\hat{O}$ is needed with the quantum numbers of a specific hadron. The operator $\hat{O}$ and $\hat{O}^{\dagger}$ have mission of annihilation and creation respectively. That is, $\hat{O}^{\dagger}$ creates a hadron from QCD vacuum when $\hat{O}$ annihilates the hadron to the vacuum state. If the sink operator ($\hat{O}$) is operated with zero momentum, we reach the formula [6]:

$$C(n_t) \equiv \langle O(\mathbf{0}, n_t)\bar{O}(\mathbf{0}, 0)\rangle = \sum_k \langle 0|\hat{O}|k\rangle\langle k|\hat{O}^{\dagger}|0\rangle e^{-n_t E_k}, \tag{3.1}$$

where E_n is discretized. If the correlation of the operators annihilates and fluctuates around a plateau, then it gives information about the ground state energy of corresponding particle. Since zero-momentum source method is used, excited states do not contribute to total energy of the particle, we reach low-lying energy values as $E_n = m$.

In order to extract the mass spectrum and the ground state energy, we plot a graph which behaves as a logarithmic function. Due to that result of the correlation function ends up with an exponential form, it is useful to plot a graph in logarithmic form to analyze the conclusions more appropriately.

Furthermore, we use a relation between correlation function for sequential n_t values, called *effective mass* as

$$m_{eff}(n_t + \frac{1}{2}) = \ln\left(\frac{C(n_t)}{C(n_t+1)}\right), \tag{3.2}$$

the correlator $C(n_t)$ is suppressed by the ground state energy quickly, hence, an *effective mass plateau* emerges.

3.2 Electromagnetic Form Factor

The electromagnetic form factor depicts the spatial distribution of both current and electric charge inside the baryon. Hence, electromagnetic form factors provide information about the structure of the hadron, determining the form factor is useful to get a result about the size and shape of the baryons, as well as understanding the baryon structure in terms of the quark-gluon degrees of freedom [25–27]. We will give more details about basis of finding the form factor.

3.2.1 Lattice formulation

In this section, we attempt to calculate the electromagnetic form factor of the Ξ_c and Ξ_c' baryons. Therefore, we should start with evaluating the transition matrix element [28, 29]:

$$\langle \mathscr{B}(p)|V_\mu|\mathscr{B}(p')\rangle = \bar{u}(p)[\gamma_\mu F_{1,\mathscr{B}}(q^2) + i\frac{\sigma_{\mu\nu}q^\nu}{2m_{\mathscr{B}}}F_{2,\mathscr{B}}(q^2)]u(p), \tag{3.3}$$

where $m_{\mathscr{B}}$ denotes the baryon mass, $u(p)$ is the Dirac spinor and $q_\mu = p'_\mu - p_\mu$ is the transferred momentum. $V_\mu = \sum_q e_q \bar{q}(x)\gamma_\mu q(x)$ is electromagnetic vector current where q is summed over related quark content [30–32]. Furthermore, $F_{1,\mathscr{B}}(q^2)$ and $F_{2,\mathscr{B}}(q^2)$ can be expressed in terms of Sachs electric and magnetic form factors as follows:

$$G_{\mathscr{E},\mathscr{B}} = F_{1,\mathscr{B}}(q^2) + \frac{q^2}{4m_{\mathscr{B}}^2}F_{2,\mathscr{B}}(q^2), \tag{3.4}$$

$$G_{\mathscr{M},\mathscr{B}} = F_{1,\mathscr{B}}(q^2) + F_{2,\mathscr{B}}(q^2). \tag{3.5}$$

3.2.2 Correlation function and ratio

The two point and three point correlation functions are described respectively as:

$$\langle F^{\mathscr{B}\mathscr{B}}(t;\mathbf{p};\Gamma_4)\rangle = \sum_x e^{-i\mathbf{p}x}\Gamma_4^{\alpha\alpha'}\langle 0|T[\eta_{\mathscr{B}}^{\alpha}(x)\bar{\eta}_{\mathscr{B}}^{\alpha'}(0)]|0\rangle. \tag{3.6}$$

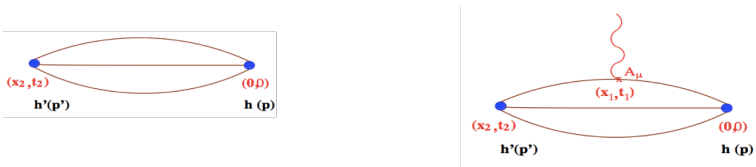

Figure 3.1 : Diagram of the two and three point correlations [7].

$$\langle F^{\mathscr{B}\mathscr{V}_\mu\mathscr{B}}(t_2,t_1;\mathbf{p}',\mathbf{p};\Gamma_4)\rangle = -i\sum_{x_1,x_2} e^{-i\mathbf{p}x_2}e^{i\mathbf{q}x_1}\Gamma^{\alpha\alpha'}\langle 0|T[\eta^{\alpha}_{\mathscr{B}}(x_2)V_\mu(x_1)\bar{\eta}^{\alpha'}_{\mathscr{B}}(0)]|0\rangle, \tag{3.7}$$

where $\Gamma_i = \gamma_i\gamma_5\Gamma_4$ and $\Gamma_4 \equiv (1+\gamma_4)/2$. We are able to construct the ratio in terms of the two point and three point correlation function. Then, using the ratio we can extract the baryon electric and magnetic form factor. The equation $R(t_2,t_1;\mathbf{p}',\mathbf{p};\Gamma;\mu)$ is expressed explicitly as [33],

$$\frac{\langle F^{\mathscr{B}\mathscr{V}_\mu\mathscr{B}}(t_2,t_1;\mathbf{p}',\mathbf{p};\Gamma_4)\rangle}{\langle F^{\mathscr{B}\mathscr{B}}(t;\mathbf{p}';\Gamma_4)\rangle}\left[\frac{\langle F^{\mathscr{B}\mathscr{B}}(t_2-t_1;\mathbf{p};\Gamma_4)\rangle\langle F^{\mathscr{B}\mathscr{B}}(t_1;\mathbf{p}';\Gamma_4)\rangle\langle F^{\mathscr{B}\mathscr{B}}(t_2;\mathbf{p}';\Gamma_4)\rangle}{\langle F^{\mathscr{B}\mathscr{B}}(t_2-t_1;\mathbf{p}';\Gamma_4)\rangle\langle F^{\mathscr{B}\mathscr{B}}(t_1;\mathbf{p};\Gamma_4)\rangle\langle F^{\mathscr{B}\mathscr{B}}(t_2;\mathbf{p};\Gamma_4)\rangle}\right]^{1/2}, \tag{3.8}$$

If $t_2 - t_1$ and $t_1 \gg$ a, then the ratio reduces to the simpler form,

$$R(t_2,t_1;\mathbf{p}',\mathbf{p};\Gamma;\mu) \xrightarrow[\mathrm{t_2-t_1\gg a}]{\mathrm{t_1\gg a}} \Pi(\mathbf{p}',\mathbf{p};\Gamma;\mu). \tag{3.9}$$

We arrange the ratios with appropriate Lorentz orienting of μ and projection of Γ in terms of forms factors $G_{E,\mathscr{B}}(q^2)$ and $G_{M,\mathscr{B}}(q^2)$ as ,

$$\Pi(\mathbf{0},\text{-}\mathbf{q};\Gamma_4;\mu=4) = \left[\frac{(E_{\mathscr{B}}+m_{\mathscr{B}})}{2E_{\mathscr{B}}}\right]^{1/2} G_{E,\mathscr{B}}(q^2), \tag{3.10}$$

$$\Pi(\mathbf{0},\text{-}\mathbf{q};\Gamma_j;\mu=i) = \left[\frac{1}{2E_{\mathscr{B}}(E_{\mathscr{B}}+m_{\mathscr{B}})}\right]^{1/2} \varepsilon_{ijk}q_k G_{M,\mathscr{B}}(q^2). \tag{3.11}$$

When q is equal to zero $G_{E,\mathscr{B}}(0)$ factor gives us the electric charge and $G_{M,\mathscr{B}}(0)$ extract the magnetic moment of the baryon. The magnetic moment is described in nuclear magnetons as follows :

$$\mu_{\mathscr{B}} = G_M(0)\left(\frac{m_N}{m_{\mathscr{B}}}\right)\mu_N, \tag{3.12}$$

where m_N is the nuclear mass and μ_N is the nuclear magnetic moment.

3.3 Techniques For Analyzing Data

In order to handle a data set, Jackknife is one of the most useful methods. This method not only eliminates bias parameters but also constructs sample subsets from original data set. Suppose that we have a data set with size of N and there is a θ parameter which is observable. Furthermore, the value of the observable calculated for the data set is called $\hat{\theta}$. Then, variance for θ,

$$\sigma_{\hat{\theta}} \equiv \frac{N-1}{N} \sum_{n=1}^{N} (\theta_n - \hat{\theta})^2. \tag{3.13}$$

The square root of variance gives approximately standard deviation of $\hat{\theta}$. Thus, the biased estimator is computed as $\langle\theta\rangle = \hat{\theta} \pm \sigma_{\hat{\theta}}$. Now, we try to remove bias from the estimator $\langle\theta\rangle$. Alternatively, bias may be calculated from,

$$\tilde{\theta} \equiv \frac{1}{N} \sum_{n=1}^{N} \theta_n, \tag{3.14}$$

which concluding to $\tilde{\theta} - (N-1)(\tilde{\theta} - \hat{\theta})$ for the unbiased estimator for $\langle\theta\rangle$. Ultimately, a favorable property of the jackknife methods is the fact that it can be used for the finding out the statistical error for fitted quantities. In addition, it does not need any complicated data propagation for data analysis.

3.4 Simulation Details

We employ lattices of size $16^3 \times 32$ with two flavors of dynamical quarks and the gauge configurations we use have been generated by the CP-PACS collaboration [17] with the renormalization group improved gauge action and the mean-field improved clover quark action. We use the gauge configurations at $\beta = 1.95$ with the clover coefficient $c_{SW} = 1.530$, which give a lattice spacing of $a = 0.1555(17)$ fm (a^{-1}= 1.267 GeV) as determined from the ρ-meson mass. The simulations are carried out with one hopping parameter for the sea and the u, d valence quarks, κ_{sea} , $\kappa_{u,d}$ =

0.1410 which corresponds to quark mass of $\sim$ 35 MeV, and we use 50 such gauge configurations, respectively. The hopping parameter for the s valence quark is fixed to $\kappa_{s,val}$= 0.1393 so that the Kaon mass is reproduced, which corresponds to a quark mass of 90 MeV. We employ smeared source and smeared sink, which are separated by 8 lattice units in the temporal direction. Source and sink operators are smeared in a gauge-invariant manner with the root mean square radius of 0.6 fm. All the statistical errors are estimated via the jackknife analysis.

The baryon interpolating-field for Ξ_c' and Ξ_c respectively are,

$$\eta_{\Xi_c'} = \frac{1}{\sqrt{2}}\varepsilon_{abc}\left[\left(u_a^T(C\gamma_5)c_b\right)s_c + \left(s_a^T(C\gamma_5)c_b\right)u_c\right], \tag{3.15}$$

$$\eta_{\Xi_c} = \frac{1}{\sqrt{6}}\varepsilon_{abc}\left[2(s_a^T(C\gamma_5)u_b)c_c + (s_a^T(C\gamma_5)c_b)u_c - (d_a^T(C\gamma_5)c_b)s_c\right]. \tag{3.16}$$

4. CHAPTER 4

4.1 Results

4.1.1 Mass spectrum

After plotting the convenient ratios of correlation functions, we seek for a *plateau*. Due to the fact that suitable ratio values tend to stay constant according to time, we figure out a constant fit value (see Appendix A.). This procedure is followed for both of the baryons we consider. We obtain the masses as in figure 4.1. and 4.2. We give our fitted results for the baryon masses in Table 4.1.

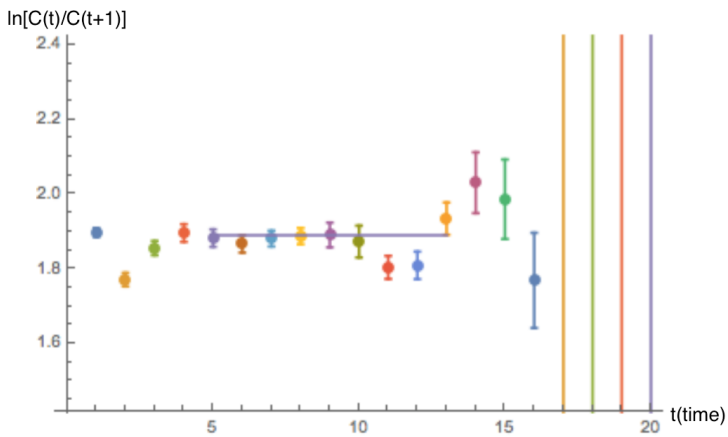

Figure 4.1 : Effective mass plot of Ξ_c, black horizontal line indicates the fit region.

Table 4.1 : Mass and fit values.

baryon	mass (GeV)	fit value	experimental results
Ξ_c	2375.7 $\pm$12.8	1.8618 $\pm$ 0.0159	2467.8 $\pm$ 0.6
Ξ_c'	2512.6 $\pm$10.8	1.9691 $\pm$ 0.0180	2575.6 $\pm$ 3.1

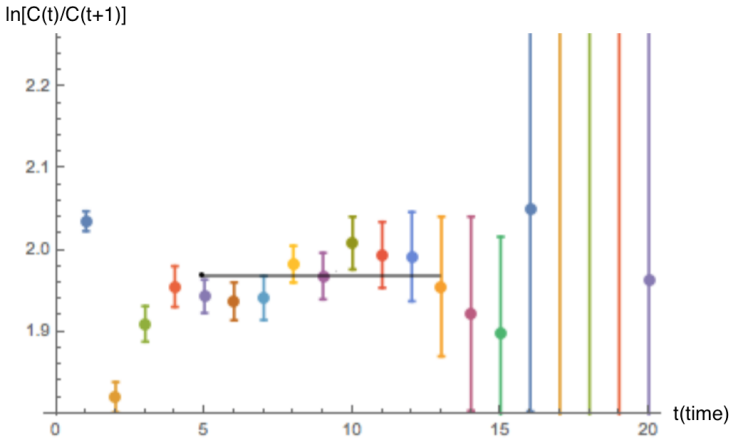

Figure 4.2 : Effective mass plot of Ξ_c', black horizontal line indicates the fit region.

4.1.2 Electric form factor

Electric form factor plots give us electric charge of Ξ_c and Ξ_c' baryons at zero momentum. In Figure 4.3 and Figure 4.4, the electric charge is 0 for *dsc* combination. In Figure 4.5 and Figure 4.6, electric form factor gives +1 at zero momentum for *usc* combination. Furthermore, the electric form factor provides more valuable information to understand inner structure of baryons at non-zero momentum since it is possible to encounter quarks directly instead of composite structure of baryon. Because of electric charge of quarks, the electric form factor fluctuates for different momentum values.

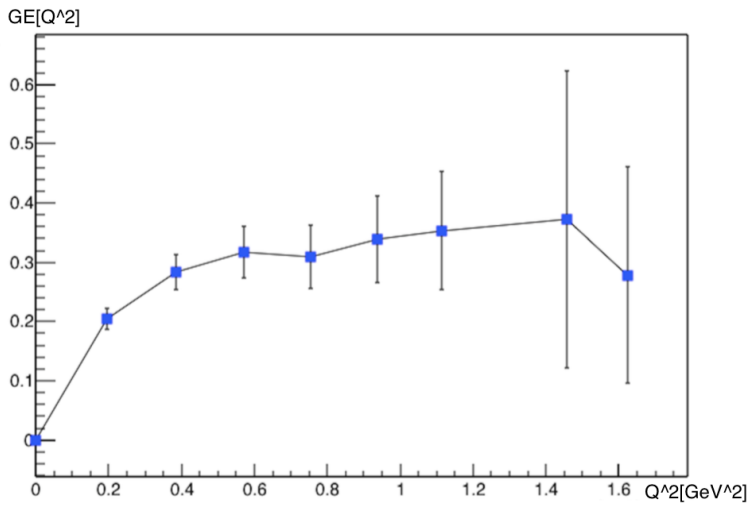

Figure 4.3 : Electric form factor of $\Xi_c(dsc)$.

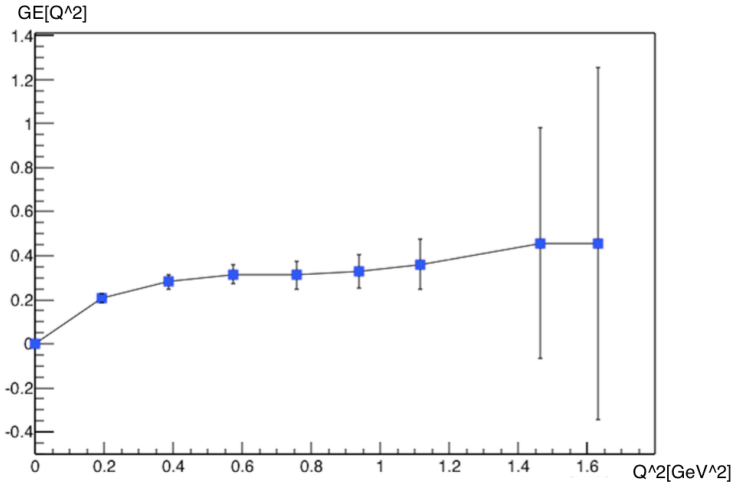

Figure 4.4 : Electric form factor of $\Xi_c'(dsc)$.

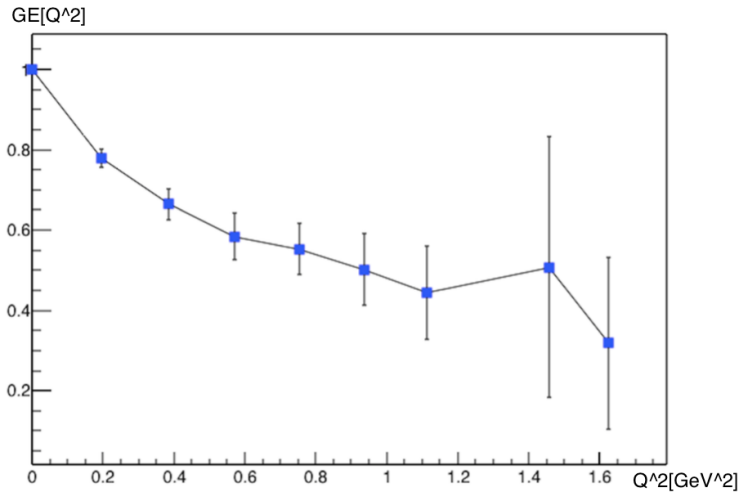

Figure 4.5 : Electric form factor of $\Xi_c(usc)$.

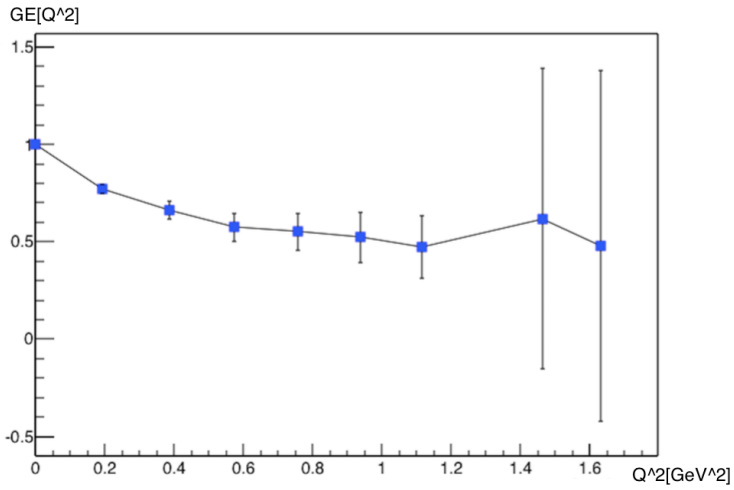

Figure 4.6 : Electric form factor of $\Xi_c'(usc)$.

4.1.3 Magnetic form factor

It is also instructive to investigate the magnetic form factor of Ξ_c and Ξ_c' to discover dynamic of baryons and individual contributions of quarks. For *usc* and *dsc* combinations, the magnetic form factors are plotted in Figure 4.7, Figure 4.8, Figure 4.9 and Figure 4.10 with respect to different momentum. However, we can not measure directly magnetic form factors at zero momentum due to momentum contribution as denoted in formula 3.11. Therefore, it is reasonable to make extrapolation over magnetic moment values to figure out $G_M(0)$. However, $G_M(0)$ is represented in Table 4.3. for *usc* and *dsc* combinations of Ξ_c and Ξ_c' baryons.

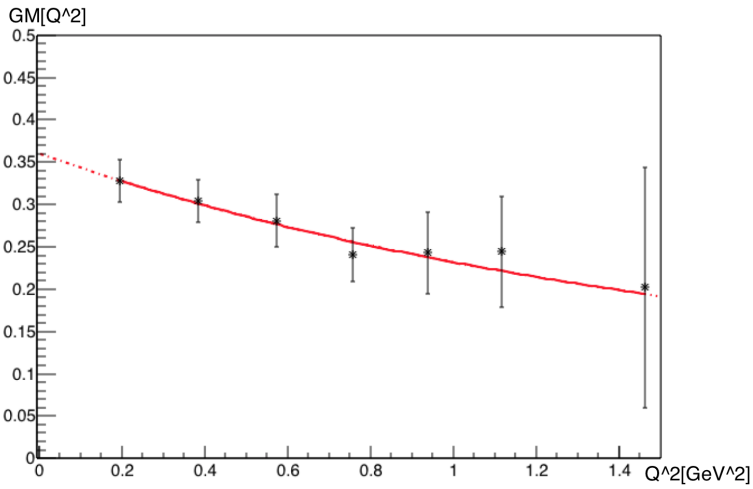

Figure 4.7 : Magnetic form factor of $\Xi_c(dsc)$.

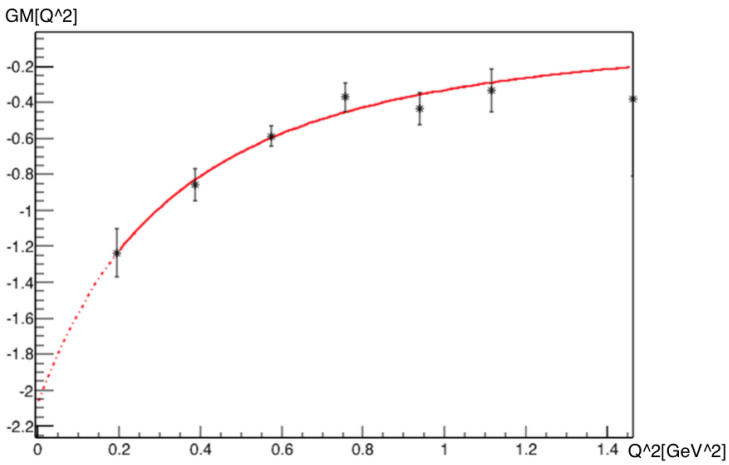

Figure 4.8 : Magnetic form factor of $\Xi_c'(dsc)$.

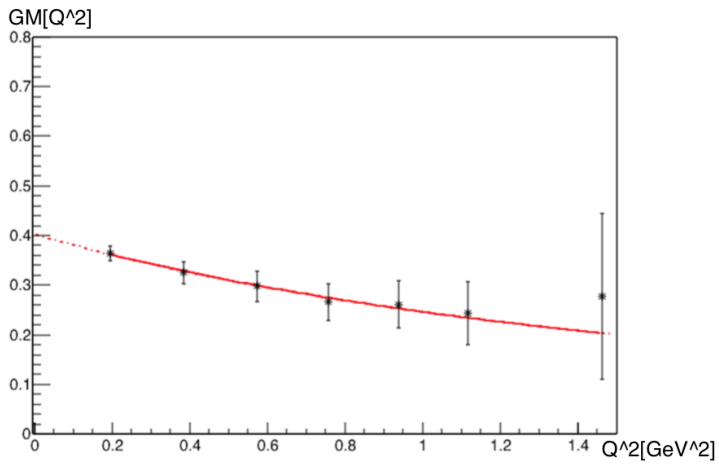

Figure 4.9 : Magnetic form factor of $\Xi_c(usc)$.

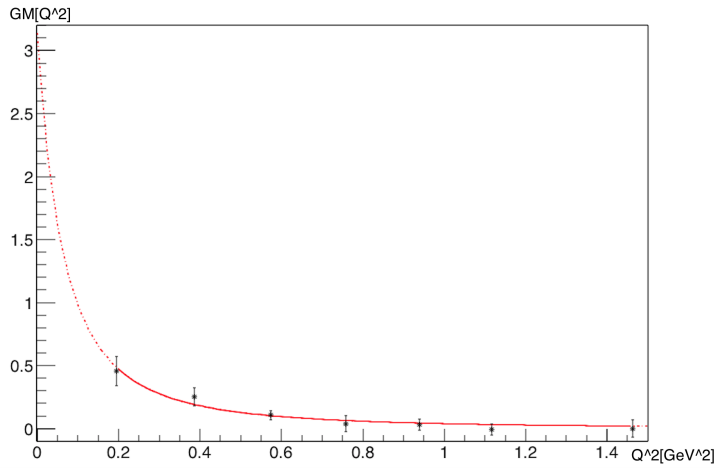

Figure 4.10 : Magnetic form factor of $\Xi_c'(usc)$.

It is convenient to evaluate magnetic moment of baryons throughout using $G_M(0)$ and Table 4.3 represents magnetic moments of baryons in terms of nuclear magneton.

Table 4.2 : Magnetic form factor of Ξ_c and Ξ_c' at zero momentum.

baryon	GM(0)
Ξ_c(dsc)	0.361 $\pm$0.029
Ξ_c'(dsc)	-2.072 $\pm$ 0.300
Ξ_c(usc)	0.403 $\pm$ 0.022
Ξ_c'(usc)	3.121 $\pm$ 1.229

As mentioned in Chapter 1, spins of the light quarks in Ξ_c baryon are anti-aligned while spins of the light quarks in Ξ_c' are aligned. According to magnetic moments of Ξ_c and Ξ_c', it can be said that the anti-aligned quark pair does not contribute to magnetic moment of Ξ_c baryon and charm quark is getting more important. It

can be seen by the differences between Ξ_c and Ξ_c' for usc and dsc configurations. Furthermore, u and d quarks have a significant role when they are aligned to s quark in Ξ_c' baryons since their contributions are dominant on magnetic moment of baryons as indicated in Table 4.2. The results of magnetic moments of Ξ_c and Ξ_c' are given in natural units.

4.2 Discussion of Errors

Systematical errors may be originated from different causes. They are able to affect simulation results significantly. First of all, lattice spacing a has very significant role for discretizing action, space-time and wave functions since they are discretized with $\mathscr{O}(a)$. Furthermore, it is suspicious to use the same fermionic action for u, s and c quarks. We assume that the lattices which have lattice spacing $a = 0.1555(17)$ result in small discretization errors.

5. CONCLUSION

We have evaluated mass spectrum of Ξ_c and Ξ_c' by starting with the *ab inito* LQCD method.

In the thesis, we have obtained discretization of the action of QCD which is the fundamental characteristic of Lattice QCD method. For this discretization procedure, the plaquette and link variable expressions emerge to ensure the gauge invariance. After this stage, we extract the mass spectrum of the particles separately from correlation function,

$$C(n_t) \equiv \langle O(\mathbf{0}, n_t)\bar{O}(\mathbf{0}, 0)\rangle = \sum_k \langle 0|\hat{O}|k\rangle\langle k|\hat{O}^\dagger|0\rangle e^{-n_t E_k}. \tag{5.1}$$

Then, we computed numerical part of calculation by simulation and perform analysis techniques to get rid of both bias and big errors. The simulations are run on $16^3 \times 32$ sized lattices with lattice spacing $a = 0.1412$ fm. We select the plateau region after plotting suitable ratio values and obtain the masses in GeV unit.

Additionally, we have investigated the electromagnetic form factors of Ξ_c and Ξ_c' hadrons. Using the evaluated mass spectrum and Sachs equation we find the form factors. Especially, understanding structure of charmed baryons is crucial to get an idea how heavy quark baryons interact. Ξ_c and Ξ_c' baryons have one heavy quark (c) and two light quarks (u or d and s), the electromagnetic form factors present precious information about interactions between the quarks inside a heavy baryon. We plot the electric and magnetic form factor with respect to two different quark contents as follows: dsc and usc. Then, we calculated magnetic moments of Ξ_c and Ξ_c' baryons and see the effect of spin alignment of light quarks on magnetic moment of baryons. Calculations are performed in ROOT and Mathematica.

REFERENCES

[1] **Edwards, R.G. and Joo, B.** (2005). The Chroma software system for lattice QCD, *Nucl. Phys. Proc. Suppl.*, *140*, 832, [,832(2004)], `hep-lat/0409003`.

[2] **Bethke, S.** (2007). Experimental tests of asymptotic freedom, *Prog. Part. Nucl. Phys.*, *58*, 351–386, `hep-ex/0606035`.

[3] **Hayano, R.S. and Hatsuda, T.** (2010). Hadron properties in the nuclear medium, *Rev. Mod. Phys.*, *82*, 2949, `0812.1702`.

[4] **Blossier, B.**, **Boucaud, P.**, **Brinet, M.**, **De Soto, F.**, **Du, X.**, **Morenas, V.**, **Pene, O.**, **Petrov, K. and Rodriguez-Quintero, J.** (2012). The Strong running coupling at τ and Z_0 mass scales from lattice QCD, *Phys. Rev. Lett.*, *108*, 262002, `1201.5770`.

[5] **Olive, K.A.** *et al.* (2014). Review of Particle Physics, *Chin. Phys.*, *C38*, 090001.

[6] **Gattringer, C. and Lang, C.B.** (2010). *Quantum chromodynamics on the lattice*, Springer-Verlag Berlin Heidelberg.

[7] **Alexandrou, C.**, **Koutsou, G.**, **Leontiou, T.**, **Negele, J.W. and Tsapalis, A.** (2007). Axial Nucleon and Nucleon to Delta form factors and the Goldberger-Treiman Relations from Lattice QCD, *Phys. Rev.*, *D76*, 094511, [Erratum: Phys. Rev.D80,099901(2009)], `0706.3011`.

[8] **Drechsel, D. and Walcher, T.** (2008). Hadron structure at low Q**2, *Rev. Mod. Phys.*, *80*, 731–785, `0711.3396`.

[9] **Ioffe, B.L.** (2006). QCD at low energies, *Prog. Part. Nucl. Phys.*, *56*, 232–277, `hep-ph/0502148`.

[10] **Reinders, L.J.**, **Rubinstein, H. and Yazaki, S.** (1985). Hadron Properties from QCD Sum Rules, *Phys. Rept.*, *127*, 1.

[11] **Weinberg, S.** (1979). Phenomenological Lagrangians, *Physica*, *A96*, 327–340.

[12] **Gasser, J. and Leutwyler, H.** (1985). Chiral Perturbation Theory: Expansions in the Mass of the Strange Quark, *Nucl. Phys.*, *B250*, 465–516.

[13] **Wilson, K.G.** (1974). Confinement of Quarks, *Phys. Rev.*, *D10*, 2445–2459, [,45(1974)].

[14] **Wilson, K.G.** (1974). Quark Confinement., *Conf. Proc.*, *C7406241*, 125–147.

[15] **Wilson, K.G.** (1974). Quark Confinement, *Marseille Colloq.,1974:125*, p.125.

[16] **Alexandrou, C.** (2009). Baryon structure from Lattice QCD, *Chin. Phys.*, *C33*, 1093–1101, 0906.4137.

[17] **Aoki, S.** *et al.* (2009). 2+1 Flavor Lattice QCD toward the Physical Point, *Phys. Rev.*, *D79*, 034503, 0807.1661.

[18] **Bali, G.S.** (2001). QCD forces and heavy quark bound states, *Phys. Rept.*, *343*, 1–136, hep-ph/0001312.

[19] **Day, J.P.** (2013). Approaches to non-perturbative problems in hadron physics, *Ph.D. thesis*, Graz U., http://media.obvsg.at/p-AC10927035-2001.

[20] **Pérez-Rubio, P.**, **Collins, S. and Bali, G.S.** (2015). Charmed baryon spectroscopy and light flavor symmetry from lattice QCD, *Phys. Rev.*, *D92*(3), 034504, 1503.08440.

[21] **Davies, C.** (2013). Precise Determination of the Charm Quark Mass, *Proceedings, 6th International Workshop on Charm Physics (Charm 2013)*, https://inspirehep.net/record/1267659/files/arXiv:1312.1556.pdf, 1312.1556.

[22] **Anselmino, M.**, **Lichtenberg, D.B. and Predazzi, E.** (1990). Effect of Quark Color - Hyperfine Interactions on Baryon Masses, *Z. Phys.*, *C48*, 605–612.

[23] **Franklin, J.** (1997). Mixing of Xi(c) - Xi(c)-prime baryons, *Phys. Rev.*, *D55*, 425–426, hep-ph/9606326.

[24] **Lesiak, T.** *et al.* (2005). Measurement of masses and branching ratios of Xi+(c) and Xi0(c) baryons, *Phys. Lett.*, *B605*, 237–246, [Erratum: Phys. Lett.B617,198(2005)], hep-ex/0409065.

[25] **Hagler, P.** (2010). Hadron structure from lattice quantum chromodynamics, *Phys. Rept.*, *490*, 49–175, 0912.5483.

[26] **Constantinou, M.** (2015). Hadron Structure, *PoS*, *LATTICE2014*, 001, 1411.0078.

[27] **Green, J.** (2016). Hadron Structure from Lattice QCD, *AIP Conf. Proc.*, *1701*, 040007, 1412.4637.

[28] **Erkol, G.**, **Oka, M. and Takahashi, T.** (2010). Axial Charges of Octet Baryons in Two-flavor Lattice QCD., *Phys. Lett.*, *B686*, 36–40.

[29] **Can, K.U.**, **Kusno, A.**, **Mastropas, E.V. and Zanotti, J.M.** (2015). Hadron Structure on the Lattice, *Lect. Notes Phys.*, *889*, 69–105.

[30] **Can, K.U.**, **Erkol, G.**, **Oka, M.**, **Ozpineci, A. and Takahashi, T.** (2015). Look inside charmed-strange baryons from lattice QCD, *Phys. Rev.*, *D92*(11), 114515, 1508.03048.

[31] **Wilcox, W.**, **Draper, T. and Liu, K.F.** (1992). Chiral limit of nucleon lattice electromagnetic form-factors, *Phys. Rev.*, *D46*, 1109–1122, hep-lat/9205015.

[32] **Can, K.U.**, **Erkol, G.**, **Isildak, B.**, **Oka, M. and Takahashi, T.T.** (2014). Electromagnetic structure of charmed baryons in Lattice QCD, *JHEP*, *05*, 125, 1310.5915.

[33] **Alexandrou, C.**, **Brinet, M.**, **Carbonell, J.**, **Constantinou, M.**, **Harraud, P.A.**, **Guichon, P.**, **Jansen, K.**, **Korzec, T. and Papinutto, M.** (2011). Nucleon electromagnetic form factors in twisted mass lattice QCD, *Phys. Rev.*, *D83*, 094502, 1102.2208.

APPENDICES

APPENDIX A : Mass plots of Ξ_c and Ξ_c' baryons

0pt

APPENDIX A

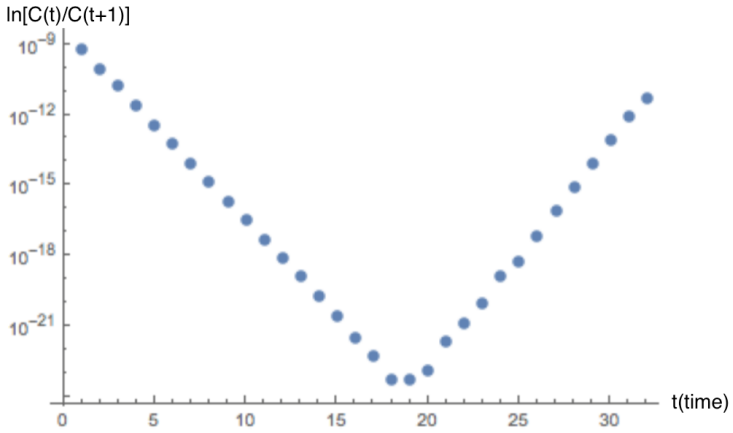

Figure A.1 : Linear mass plot of Ξ_c.

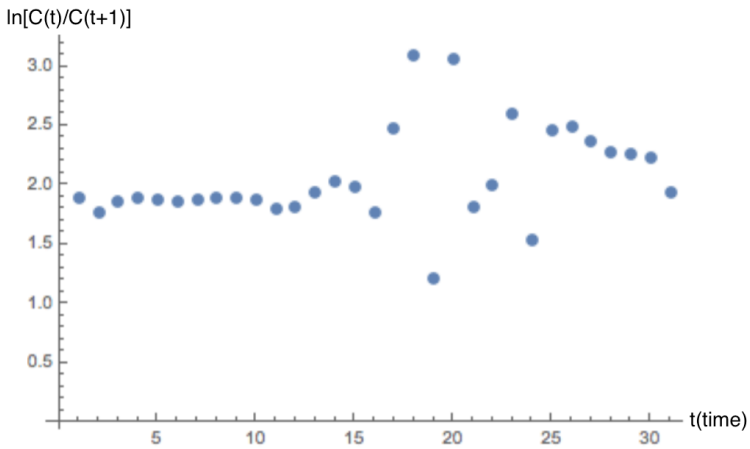

Figure A.2 : Mass spectrum plot of Ξ_c.

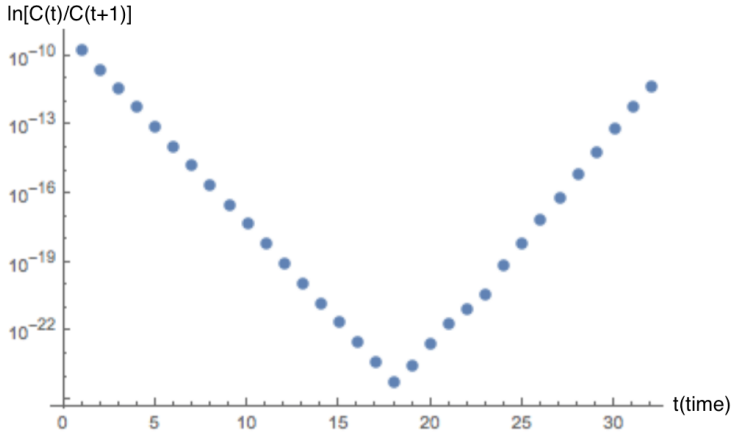

Figure A.3 : Linear mass plot of Ξ_c'.

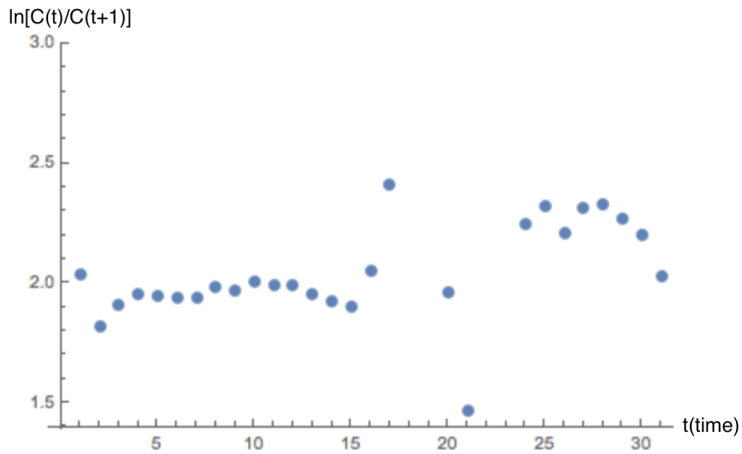

Figure A.4 : Mass spectrum plot of Ξ_c'.

CURRICULUM VITAE

Name Surname: Onur Karayalçın

Place and Date of Birth: Sivas - 10.05.1991

Adress: Fizik Mühendisliği Bölümü, Fen Edebiyat Fakültesi,
Ayazağa Kampüsü, İstanbul Teknik Üniversitesi, Sarıyer

E-Mail: karayalcino@itu.edu.tr - onurkarayalcn@gmail.com

B.Sc.: Physics Engineering, Hacettepe University

M.Sc.: Physics Engineering, Istanbul Technical University